The Next Wave: Buoy Arrays for Deterministic Wave Prediction in Real-time

Jim Thomson
Applied Physics Laboratory
University of Washington
Seattle, WA (USA)
jthomson@apl.washington.edu

Alex Fisher
Department of Ecology
State of Washington
Lacey, WA (USA)
afis461@ecy.wa.gov

Curtis J. Rusch
Applied Physics Laboratory
University of Washington
Seattle, WA (USA)
curusch@uw.edu

***Abstract*—This work uses sparse arrays of ocean wave buoys to create a linear reconstruction of the sea surface and provide deterministic wave predictions at a future time and nearby position (i.e., within a few wavelengths). The predictions are constrained to be within the statistics of recently observed waves. This recently established method is applied in post-processing at two distinct projects related to 1) a wave energy converter and 2) an offshore wind platform. The conditions range from scale-model tank testing to an operational open-ocean wind farm. Relative to a conventional statistical forecasting with random waves, the method achieves at least 60% improvement in prescribing the next several waves arriving at a given target location. Work is ongoing to implement this method in realtime, using radio modems to transmit raw motion data (5 Hz sampling) from the buoy array to a central node that continually updates a 30-second prediction window with less than 1-second latency. The deterministic wave predictions can be used to improve control strategies for platforms at sea, with improvements in efficiency and reductions in dynamic loads.**

***Index Terms*—ocean surface waves, wave prediction, real-time control**

I. Introduction

Many applications in marine and offshore engineering require knowledge of the sea state. Traditionally, this information has been in the form ocean wave statistics, such as the significant wave height, peak wave period, and dominant wave direction. Scalar and directional wave spectra also are commonly used. The spectra provide further information on the various scales of wave motion, but the information remains statistical. Wave phase is not retained in most spectral representations, nor is it included in spectral wave forecasts systems such as WAVEWATCH III or SWAN. Thus, conventional wave observations and forecasts do not provide information on the timing or amplitude of individual waves.

Recent work has shown that deterministic predictions of individual ocean waves are not only possible, but also practical and achievable, using arrays of wave measurement buoys [1]. We present three real-world applications of this method and evaluate the predictive performance relative to purely statistical (i.e., random phase) representations of the wave field. Each application is restricted to space-time prediction zones within a few wavelengths or wave periods of the buoy array.

Funding provided by the U.S. Navy (Naval Facilities Engineering Systems Command) and by the U.S. Department of Energy Advanced Research Projects Arm (ARPA-E)

II. Methods

The methods are presented in detail within [1] and are only reviewed here. We refer to the methodology as The Next Wave and provide public code at https://github.com/SASlabgroup/TheNextWave for general usage. Additional practical documentation is include in the GitHub repository.

The underlying assumption is a sea surface that can be described as a linear superposition of wave components, which can be estimated from coherent space-time observations [2]. The assumption of linearity makes the method computationally efficient (and thus fast enough for realtime applications), but it removes any ability to describe the evolution of the waves. It is purely a propagation and superposition method. Thus, the method is intended for short space and time scales (e.g., a few wavelengths and a few wave periods).

The sea surface elevation $\eta(x, y, t)$ at any position (x, y) and time t is given by

$$\eta = \mathbf{PB}, \tag{1}$$

where B is a $N \times 1$ vector of unknown complex amplitudes (i.e., amplitudes and phases), and $\mathbf{P}$ is a $M \times N$ propagator matrix that describes the projection of each wave component in space and time. Using vector notation for position $\mathbf{x}$ and wavenumber $\mathbf{k}$, this matrix is thus

$$P_{m,n} = \exp\left(i\left(\mathbf{x}_m \cdot \mathbf{k}_n - \omega_n t\right)\right), \tag{2}$$

where ω is the radian frequency and the linear dispersion relation is $\omega = gk\tanh(kd)$ in a given water depth d.

When measurements of horizontal velocities are available, $\mathbf{P}$ can be extended to a $3M$ x N matrix

$$\begin{vmatrix} \tilde{\eta}_m \\ \tilde{u}_m \\ \tilde{v}_m \end{vmatrix} = \begin{vmatrix} \exp\left(i\Phi\right)_{m,n} \\ \frac{k_x}{k}\omega\exp\left(i\Phi\right)_{m+M,n} \\ \frac{k_y}{k}\omega\exp\left(i\Phi\right)_{m+2M,n} \end{vmatrix} \left|B_n\right| \tag{3}$$

where $\Phi = \mathbf{x}_m \cdot \mathbf{k}_n - \omega_n t_m$ and $\tilde{\eta}$, $\tilde{u}$, $\tilde{v}$ indicate predicted displacement and horizontal velocities, respectively. This provides an additional constraint on the linear superposition and reduces the sparseness of the formulation.

By inverting Eq. 3 and solving for unknown component amplitudes and phases B, a reduced-order approximation of the free surface can be projected in space and time to yield predictions of instantaneous wave conditions at a target location over a finite reconstruction horizon [3]. The inversion is sparse when using an array of only a few buoys, and it is thus important to constrain the inversion; component amplitudes are bound by observed directional wave energy distributions (i.e., conventional directional spectra from the buoys.) To simplify the code for the constrained least squares problem, the propagator matrix P is converted to a sum of sines and cosines via Euler's formula, increasing the number of unknowns from N to $2N$ and the size of the matrix to $3M \times 2N$.

The observations of η, u, v used to invert Eq. 3 are from SWIFT buoys [4] at discrete x, y, t. We use version 4 (v4) of the SWIFT buoys [5], which integrates a GPS-aided inertial motion unit (SBG Ellipse-N) with an onboard Extended Kalman Filter (EKF). The realtime EKF solutions are output at 5 Hz with precision as follows: $\Delta\eta \sim 0.05\mathrm{m}, \Delta u \sim 0.01\mathrm{m/s}, \Delta v \sim 0.01\mathrm{m/s}, \Delta x \sim 1\mathrm{m}, \Delta y \sim 1\mathrm{m}, \Delta t \sim 10^{-6}\mathrm{s}$. During method development, sparse arrays of 3 to 8 buoys were used [1]. In the applications that follow, arrays of 4 buoys are used.

The solution space is specified *a priori* based on the number of buoys available and the directional wave spectrum from the previous complete wave record (nominally every 30 minutes). To avoid fitting noise, the frequency range is limited to frequencies with energy density that is at least 5% of the peak of the spectrum and directions within $\pi/2$ of the dominant wave direction. The actual number of components used in the inversion is a subjective choice that is a trade-off of computational speed, accuracy, and robust fitting. After testing a range of options, we have settled on 40 logarithmically-spaced frequency components and 25 directional components.

The spatiotemporal prediction horizon (and prediction skill) of ocean waves is limited by the bandwidth of the wave field and span of measurements [3]. This prediction horizon is an essential consideration in designing the array of buoys, relative to the target location. The buoys should be aligned along the axis of dominant wave direction and spaced within 1-2 wavelengths of the dominant waves. Even when designed according to these guidelines, the skill of the method is a strong function of bandwidth and directional spread. A wave field that is narrower in frequency and/or direction will have a well-constrained inversion and superposition.

We use a skill metric that compares the deterministic prediction (denoted with p) with a "dummy" statistical forecast (denoted with s) that is a random phase reconstruction from the prior directional spectrum. Both are constrained by the observed statistics, but one the former has nearby amplitudes/phases and the latter is purely random. The skill metric is defined as

$$S = 1 - \frac{MSE_p}{MSE_s}, \tag{4}$$

where MSE_p, and MSE_s, are the mean square errors between the true $\eta(x, y, t)$ and the predicted (p) or statistical (s) $\eta(x, y, t)$. This skill metric requires a measure of the "true" $\eta(x, y, t)$, which usually is given by a buoy that is withheld from the inversion of Eq. 3 (i.e., data denial). The skill metric is evaluated over data records that are 512-seconds long (at 5 Hz resolution). For robust statistics, the skill score is calculated using the median value of MSE_s based on 50 random-phase realizations of the sea surface.

III. Results

Results are presented from three applications, as summarized in Table I. In the first application, wave predictions provide time-domain forcing information for analysis of power production and dynamics in a Wave Energy Converter (WEC). In the second and third applications, wave predictions provide time-domain forcing information for analysis of motions and loads in a floating wind platform. In future applications, wave predictions may be used for active control strategies to improve performance or warning systems to reduce loads under extreme (rogue) waves.

TABLE I
PROJECTS AND WAVE CONDITIONS

Project	Duration	H_s	T_p
TigerRAY wave energy converter	6 days	0.2-0.6 m	2-4 s
DigiFloat offshore wind (scale model)	20 hours	0.1-0.4 m	1-3 s
DigiFloat offshore wind (full scale)	2 months	0 - 5 m	5-14 s

A. TigerRAY wave energy converter (WEC)

The "TigerRAY" is a WEC designed by C-Power, and furnished with an integrated UUV (uncrewed underwater vehicle) by the Applied Physics Laboratory at the University of Washington (APL-UW). Several sea-trials of this system have been completed, each in a drifting mode with four SWIFT buoys tethered to the system (see Figure 1). The trials usually lasted a few hours and the wave conditions were typical of the fetch-limited conditions in Puget Sound (Washington State, USA). These wave conditions are modest ($H_s \sim 0.4$ m, $T_p \sim 3$ s) and the short-crested conditions are challenging for the prediction method, because the directional width is broad and the wavelengths are short (thus the prediction horizon is small in both space and time).

Figure 2 shows an example time series from the prediction method (using 4 buoys) and the "true " time series observed at the WEC. For this application, the "true " time series is given by an SBG Ellipse-N sensor mounted on the WEC. Given the mass and buoyancy of the WEC, the response is damped at the higher frequencies, but still representative at the dominant frequencies of the wave field ($f \sim 0.3$ Hz). Notable for this application is the symmetric usage of the method, in which the buoys down-wave of the WEC are used to reconstruct/predict the time series at the WEC in post-processing. This is valid as a post-processing method, but would clearly fail in a real-time application.

Fig. 1. Tiger Ray Wave Energy Converter and four tethered SWIFT buoys.

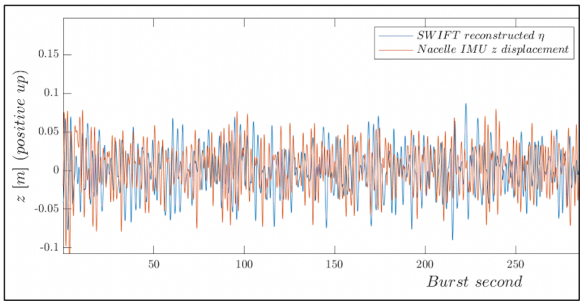

Fig. 2. Example time series of predicted and observed sea surface elevations at the Tiger Ray WEC. Skill score $S = 0.42$ (i.e., 42% improvement relative to statistical forecast).

Figure 3 shows the skill of the prediction at the WEC as defined by Eq. 4 over 45 wave records spread across three days of sea trials. Each record, or burst, of wave data is 512 seconds long. The skill is typically above 0.4, which is a 40% increase in accuracy relative to a statistical forecast, but for a single record it is negative. In this rare occasion, the prediction is actually worse than a random-phase statistical forecast. This demonstrates the importance of including a confidence metric in the predicted $\eta(x, y, t)$.

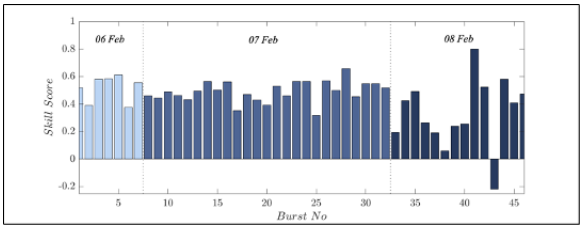

Fig. 3. Skill metric during Tiger Ray field trials in February 2023.

B. WindFloat®, scaled tank tests

The WindFloat® is a platform designed by Principle Power, Inc. to support floating offshore wind turbines. As part of a collaborative project to develop a digital twin of the WindFloat®, as series of experiments with a scaled model were conducted in the Naval Surface Warfare Center MASK wave basin at Carderock (Virginia, USA). Four SWIFT buoys were moored in the basin along with the scaled WindFloat® (Fig. 4). The 6-m spacing was designed to be similar (or less than) the wavelengths produced by the wavemakers. The statistical wave spectra and significant wave heights estimated from the SWIFT buoys agree to within 95% of the estimates from NSWC ultrasonic wave probes deployed throughout the wave tank.

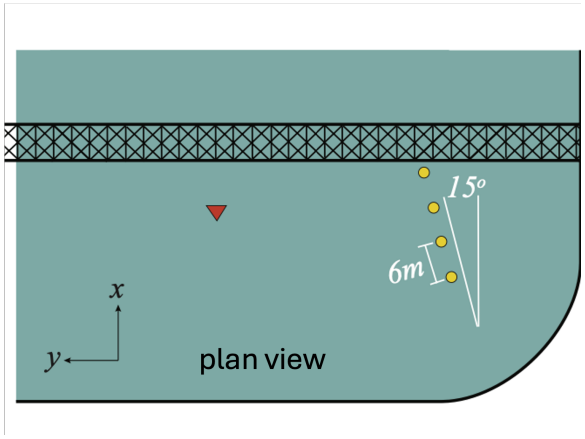

Fig. 4. Plan view of the scaled model test locations in the Carderock Wave Basin. Red triangle is the scaled model of the Wind Float platform. Yellow circles are the SWIFT buoys. The wave-maker produced waves propagating in the $+x$ direction.

The Next Wave algorithm was employed across all test conditions using three buoys, and a median skill score of 75% was determined using the fourth buoy as a data-denial groundtruth. The increase in skill score, relative to the WEC tests in the preceding section, likely is related to the long-crested waves generated in the tank. Rolling 0.5 second wave predictions were generated using a sliding window of heave measurements from the three up-wave SWIFTs. The window was 9 wave periods long. A unique challenge of the indoor tank testing was the absence of GPS signal for positioning. Instead, a laser range-finder was used to provide SWIFT locations via triangulation in the tank reference frame. The SWIFTs were constrained to watch-circles with ~ 3.5 m radius, which was an acceptable tolerance for the matrix inversion of Eq. 3. Relative to wavelength, the positional uncertainty during this test was much larger than the uncertainty of GPS positions ($\sim$ 5 m) in the open ocean (where wavelengths are $\mathcal{O}[100]$ m).

Figure 5 shows an example time series of predicted and measured wave elevations. Wave predictions slightly underpredict wave amplitude throughout the record, which is most likely due to the discretization of the solution space used in the inverse model. Determining the sensitivity of predictions to the discretization of the solution space is a direction for future method development that will require more complex analysis of tradeoffs between prediction accuracy, computational efficiency, and architecture portability.

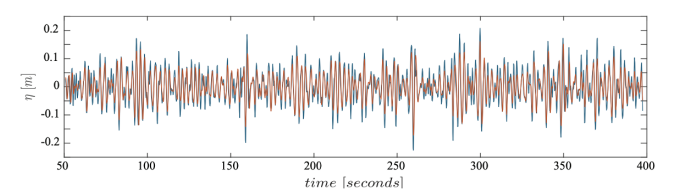

Fig. 5. Example predicted and observed time series during the Carderock Wave Basin tests. Skill score $S = 0.90$ (i.e., 90% improvement relative to statistical forecast).

C. *WindFloat®, full-scale*

Three full-scale WindFloat® platforms have been deployed 10 nautical miles off the coast of Viana do Castelo, Portugal, in the Wind Float Atlantic offshore wind farm. For two months in the autumn of 2022, four SWIFTs were moored in front a WindFloat® and used to predict incident waves. Fig. 6 shows a picture of the deployment. The SWIFTs included surface meteorological packages to record wind and air temperature, plus downward looking acoustic Doppler current profilers (ADCPs) sampling the upper 20m of the water column. The longer duration of this deployment makes it the most comprehensive test of the prediction method to date.

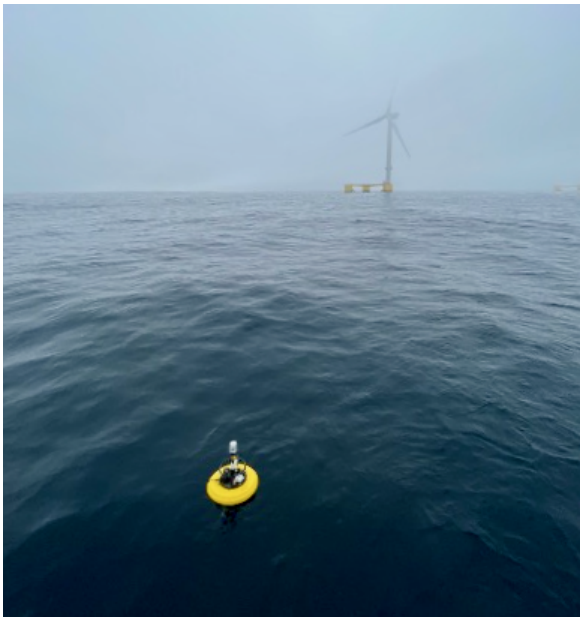

Fig. 6. Picture of SWIFT buoy moored in front of a WindFloat® platform off the coast of Portugal.

Figure 7 shows the buoy positions within the wind farm. The buoy array was deployed approximately 245 m northwest of the WindFloat®. This configuration was designed to maximize conditions in which the buoys were positioned up-wave of the platform, such that the WindFloat® would be within the prediction horizon. The buoy spacing was 115 m, based on 100-200 m wavelength in the climatology, and the moorings were designed for 30 m diameter watch circles. To achieve this watch circle in 95 m water-depth, the mooring design was two part: the lower portion was a tension mooring with a subsurface float from 10 to 95 m, and the upper portion was a 3:1 scope from 0 to 10 m depth. This design was problematic at the highest tides, when the buoy motion was restricted and the wave check factors [6] were altered. Those data are excluded from the analysis.

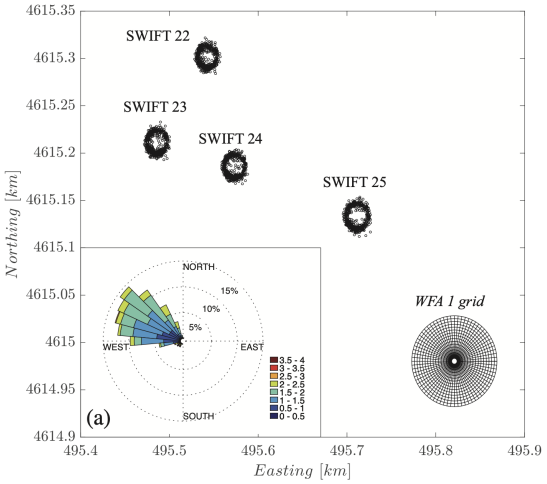

Fig. 7. Plan view of SWIFT buoy locations and Wind Float location (grid). Inset shows histogram of wave directions binned by significant wave height.

A summary of wave and wind conditions measured by the SWIFT array is shown in Fig. 8.

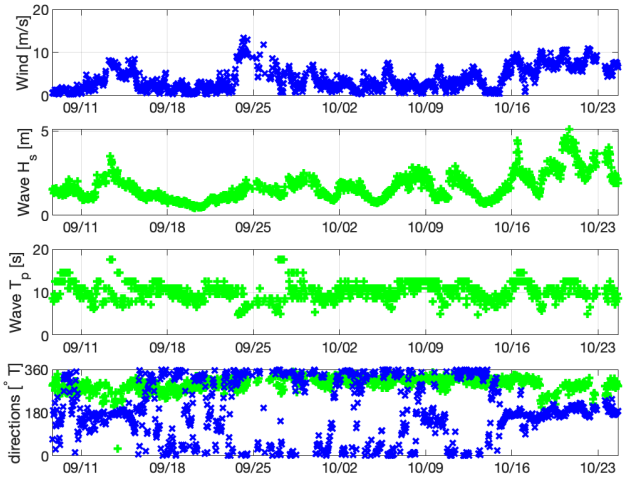

Fig. 8. Wind (blue) and wave (green) conditions during the Portugal deployment at the WindFloat® Atlantic deployment in September and October of 2022.

An example time series of predicted and observed surface elevations is shown in Fig. 9. Again, three buoys are used to predict the elevations at the fourth buoy in a data-denial experiment. Rolling 1-second wave predictions are generated 5s into the future using a sliding window of wave measurements

from the SWIFT measurement array. The window is 9 wave periods in duration.

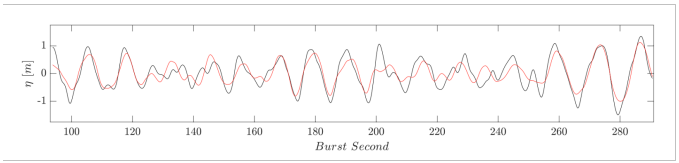

Fig. 9. Example of predicted and observed time series of sea surface elevation near the Wind Float. Skill score $S = 0.82$ (i.e., 82% improvement relative to statistical forecast).

Fig. 10 shows the skill scores during the first month of the deployment. The overall skill score was 67% when the target location was enveloped within the effective prediction zone. In nearly all cases, the linear inverse model yield predictions that were significantly more accurate than spectral forecasts with a median skill score of 49% for the whole dataset and maximum skill score of 87%.

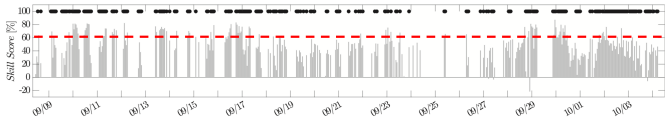

Fig. 10. Skill metric during the Wind Float field deployment. Black symbols across the top of the time series indicate conditions for which the prediction zone included the fourth buoy (and thus predictions should be most skillful).

To expand this application, sea surface predictions at the WindFloat® used the computational grid shown in Fig. 7. Using inversions from all four SWIFTs, the sea surface is predicted throughout the grid, which demonstrates the ability of the method to map the surface in space and time (not just as a single location). For a large platform like the WindFloat®, which can span a wavelength or more, such a gridded product is essential.

IV. Discussion and future application

Work is ongoing to make this method operational in real-time, with latency less than 1 second for rolling prediction windows of 10-30 seconds. The v4 SWIFTs are already equipped with radio modems (900 MHz) to transmit raw motion data (5 Hz sampling) from the buoy array to a central node/receiver. During the NSWC Carderock tank tests, the 5 Hz data was parsed onboard each SWIFT by a Sutron Xpert logger and transmitted asynchronously over a TCP/IP socket using a Digi XPress Ethernet Bridge. This has a theoretical range of 2-15 miles depending on the antenna used, and a data rate of 1.5 Mbps. At Carderock, measurements from all four SWIFTS were successfully transmitted in real-time using these modems. A set of python codes was developed for logging and plotting the transmitted data. This provides a basis for future development of a node that receives 5 Hz data and continuously updates the predictions for a particular location or grid. In the post-processing for the WindFloat® deployment, the propagator matrix can be updated with latency less than 1 second running on a single-board-computer (i.e., RaspberryPi) or standard laptop. The overall architecture is ethernet based, so integration on a wide variety of platforms should be feasible.

Essential to usage of deterministic prediction of individual waves is an accompanying confidence metric. This can be continually updated based on the conditioning of the propagator matrix. Further, realtime applications must report whether or not the target is within the prediction zone of the array, which is critical for skillful results. Future work will distill the matrix inversion and prediction zone into a single confidence metric to be continually updated with the prediction.

V. Conclusions

Recent methods for predicting individual waves based on sparse buoy arrays [1] are skillful in a series of real-world applications for Wave Energy Convertors (WECs) and offshore floating wind turbines. Other applications include warning systems for offshore oil platforms, ship-to-ship transfers at sea, and any operation with floating assets. The linear method is computationally efficient and successful over small domains and small windows of time (e.g., a few wavelengths or a few wave periods). The method is ripe for data fusion with coherent marine radars and scanning lidars, which can provide much denser spatial information but present a number of logistical challenges.

Acknowledgment

The authors thank APL-UW engineers Alex de Klerk, Emily Iseley, and Joe Talbert for preparation and maintenance of SWIFT buoys across all projects. The authors thank collaborators from Principle Power Inc. for assistance during the "DigiFloat" project, especially Pedro Baptista, Fernando Hilario, Bruce Martin, Seth Price, Samuel Rios, and Alex Sloan. The authors also thank Bradley Ling and Giovanni Rinaldi for support during the WindFloat® tank and field tests, respectively. The authors thank collaborators from C-Power for assistance during the "TigerRAY" project, especially Erik Hammagren, K. Ohearn, L. Rummel, and Zhe Zhang.

References

[1] A. Fisher, J. Thomson, and M. Schwendeman, "Rapid deterministic wave prediction using a sparse array of buoys," *Ocean Engineering*, vol. 228, p. 108871, 2021. [Online]. Available: https://www.sciencedirect.com/science/article/pii/S0029801821003061

[2] B. Connell, J. P. Rudzinsky, C. S. Brundick, W. M. Milewski, J. G. Kusters, and G. Farquharson, "Development of an environmental and ship motion forecasting system," in *Proceedings of the ASME 2015 34th International Conference on Ocean, Offshore and Arctic Engineering.*, 2015.

[3] Y. Qi, G. Wu, Y. Liu, and D. K. Yue, "Predictable zone for phase-resolved reconstruction and forecast of irregular waves," *Wave Motion*, vol. 77, pp. 195 – 213, 2018. [Online]. Available: http://www.sciencedirect.com/science/article/pii/S0165212517301518

[4] J. Thomson, "Wave breaking dissipation observed with SWIFT drifters," *Journal of Atmospheric and Oceanic Technology*, vol. 29, no. 12, pp. 1866–1882, 2012. [Online]. Available: https://doi.org/10.1175/JTECH-D-12-00018.1

[5] J. Thomson, M. Moulton, A. de Klerk, J. Talbert, M. Guerra, S. Kastner, M. Smith, M. Schwendeman, S. Zippel, and S. Nylund, "A new version of the swift platform for waves, currents, and turbulence in the ocean surface layer," in *2019 IEEE/OES Twelfth Current, Waves and Turbulence Measurement (CWTM)*, 2019, pp. 1–7.

[6] J. Thomson, J. Talbert, A. de Klerk, A. Brown, M. Schwendeman, J. Goldsmith, J. Thomas, C. Olfe, G. Cameron, and C. Meinig, "Biofouling effects on the response of a wave measurement buoy in deep water," *Journal of Atmospheric and Oceanic Technology*, vol. 32, no. 6, pp. 1281–1286, 2015/06/18 2015. [Online]. Available: http://dx.doi.org/10.1175/JTECH-D-15-0029.1